NIH Public Access
Author Manuscript
Biochemistry. Author manuscript; available in PMC 2014 October 29.

Published in final edited form as:
Biochemistry. 2013 October 29; 52(43): . doi:10.1021/bi401034q.

Mechanistic Basis for the Potent Anti-angiogenic Activity of Semaphorin 3F

Hou-Fu Guo[a], **Xiaobo Li**[a], **Matthew W. Parker**[a], **Johannes Waltenberger**[b], **Patrice M. Becker**[c,†], and **Craig W. Vander Kooi**[a,*]

[a]Department of Molecular and Cellular Biochemistry, Center for Structural Biology, University of Kentucky, Lexington, KY

[b]Division of Cardiology, Department of Cardiovascular Medicine, University Hospital Münster, Germany

[c]Division of Pulmonary and Critical Care Medicine, Johns Hopkins University School of Medicine, Baltimore, MD

Abstract

Neuropilin-1 (Nrp1), an essential type I transmembrane receptor, binds two secreted ligand families, Vascular Endothelial Growth Factor (VEGF) and class III Semaphorin (Sema3). VEGF-A and Sema3F have opposing roles in regulating Nrp1 vascular function in angiogenesis. VEGF-A functions as one of the most potent pro-angiogenic cytokines while Sema3F is a uniquely potent endogenous angiogenesis inhibitor. Sema3 family members require proteolytic processing by furin to enable competitive binding to Nrp1. We demonstrate that the furin processed C-terminal domain of Sema3F (C-furSema) potently inhibits VEGF-A dependent activation of endothelial cells. We find that this potent activity is due to unique hetero-bivalent engagement of Nrp1 by two distinct sites in the Sema3F C-terminal domain. One of the sites is the C-terminal arginine, liberated by furin cleavage, and the other is a novel upstream helical motif centered on the intermolecular disulfide. Using a novel chimeric C-furSema, we demonstrate that combining a single C-terminal arginine with the helical motif is necessary and sufficient for potent inhibition of VEGF-A binding to Nrp1. We further demonstrate that the multiple furin-processed variants of Sema3A, with altered proximity of the two binding motifs, have dramatically different potencies. This suggests that furin processing not only switches Sema3 into an activated form but, depending on the site processed, can also tune potency. These data establish the basis for potent competitive Sema3 binding to Nrp1 and provide a basis for the design of bivalent Nrp inhibitors.

Neuropilins (Nrps) are an essential cell surface receptor family [(1)]. They function with Vascular Endothelial Growth Factor Receptors (VEGFRs) in VEGF-dependent angiogenesis and with Plexin receptors in Sema3-dependent axon guidance [(2–6)]. In addition to their function in neurons, a critical role for specific Sema3 family members in physiological and pathological regulation of the cardiovascular system has been increasingly recognized [(7–9)]. For example, Sema3F is critical for maintaining an avascular outer retina, while Sema3A and Sema3E have important roles in vascular patterning [(9–12)]. In contrast, mutation and down-regulation of Sema3 family members is also observed in many types of solid tumors and has been directly correlated with tumor angiogenesis and cancer progression [(7, 13, 14)]. Indeed, restoring the expression of Sema3B and Sema3F in tumors inhibits further cancer progression *in vitro* and *in vivo* [(15–18)].

*To whom correspondence should be addressed: 741 South Limestone Ave, BBSRB B263, Lexington, KY 40536, Telephone: (859) 323-8418, Fax: (859) 257-2283, craig.vanderkooi@uky.edu.
†Present Address: Questcor Pharmaceuticals, Ellicott City, MD

NIH-PA Author Manuscript
NIH-PA Author Manuscript
NIH-PA Author Manuscript

NIH-PA Author Manuscript

NIH-PA Author Manuscript

NIH-PA Author Manuscript

Nrp serves a central role in integrating the opposing signals of VEGF and Sema3 in both physiological and pathological contexts through competitive ligand binding. The Nrp1 b1 coagulation factor domain has a conserved C-terminal arginine binding pocket that is critical for competitive VEGF and Sema3 binding [19, 20]. Alternative splicing of VEGF-A regulates Nrp1 binding [21], with the exon eight encoded C-terminal arginine residue being necessary for binding Nrp1-b1 [22]. In contrast, furin proteolysis of Sema3 is critical for regulating its ability to bind Nrp and function. Furin processing can either inactivate or activate Sema3 by processing at sites in the central or C-terminal domains, respectively. Processing in the central region of Sema3 has been primarily reported to inactivate Sema3 activity by cleaving the protein into two fragments, although the fragments may still possess activity [23–25]. Furin processing within the Sema3 C-terminal domain is critical to activate the Sema3 pro-protein by producing a C-terminal arginine, allowing competitive engagement of Nrp1-b1 [20, 26].

Multiple C-terminal arginine containing peptides and peptido-mimetics have been produced as competitive antagonists of VEGF-A/Nrp1 binding [27–29]. While functioning as inhibitors *in vitro* and *in situ*, the efficacy of these peptides and peptidomimetics suffers from limited potency ($IC_{50}\approx 10–50\ \mu M$). In contrast, endogenous Sema3F functions as a potent inhibitor of VEGF-A binding to Nrp1 [20]. However, the molecular mechanism of high-affinity Sema3F binding to Nrp1 has not been elucidated, leaving open the question of how Sema3F potently competes for Nrp1 binding.

In the present study, we demonstrate the mechanistic basis for the potency of the furin-processed C-terminal domain of Sema3F (C-furSema) (Figure 1A) *in vitro* and *in situ*. We find that C-furSema exhibits unique hetero-bivalent engagement and that this bivalent binding is essential for Nrp1. Further, different C-terminal furin processed Sema3A isoforms show a range of potencies, which correlates with the distance between the helical and C-terminal arginine binding motifs.

Experimental Procedures

C-furSema and Variant Production

Homodimeric C-furSema (GLIHQYCQGYWRHVPPSPREAPGAPRSPEPDQK KPRNRR), truncations, and point mutants were synthesized using solid phase synthesis, oxidized to produce the natural intermolecular disulfide, and purified with reversed phase high-performance liquid chromatography (HPLC) using 4.6mm*250mm, SinoChrom ODS-BP column to >95% purity (Neo-Peptide, Cambridge, MA). The monomeric C-furSema^{Mon} (GLIHQYSQGYWRHVPPSPREAPGAPRSPEPDQKKPRNRR) was produced in the same manner without oxidization. C-furSema^{Het} was produced by combining separately synthesized reduced C-furSema and C-furSema^{Helix} (GLIHQYCQGYWRH), oxidized in the presence of the excess C-furSema^{Helix}, and purified with reversed phase HPLC using 4.6mm*250mm, SinoChrom ODS-BP column to >95% purity (LifeTein, South Plainfield, NJ). All C-furSema variants were well behaved in solution and soluble to >1 mM. A dimeric construct of C-furSema^{Helix} alone showed limited solubility, with a maximal solubility in Phosphate Buffered Saline (PBS) of 20μM, and no ability to inhibit VEGF-A binding up to the limit of solubility.

Protein and peptide concentrations were determined using OD_{280} measured on a Nanodrop 1000 (Thermo Fisher Scientific, Wilmington, DE).

NIH-PA Author Manuscript

NIH-PA Author Manuscript

NIH-PA Author Manuscript

In situ inhibition assays

Porcine aortic endothelial (PAE) cells stably overexpressing VEGFR-2 and Nrp1 were utilized to measure the ability of C-furSema to block VEGF-A activation of VEGFR-2 [30]. PAE cells were grown in F12 medium (Invitrogen, Grand Island, NY) supplemented with 10% Fetal Bovine Serum (FBS) (Invitrogen, Grand Island, NY) and 1% Pen/Strep in 6-well cell culture plates to 70% confluence. Cells were then serum starved for 16 hours in Endothelial Cell Basal Growth Medium-2 (EBM-2) (Lonza, Walkersville, MD). C-furSema samples were resuspended in EBM-2, added at a final concentration of 10 μM, and incubated for 90 minutes at 37°C. Cells were then stimulated with 100 ng/ml VEGF-A (R&D Systems, Minneapolis, MN) for 3 minutes. After 3 minutes, media was removed and cells solubilized in RIPA buffer supplemented with phosphatase and protease inhibitor (Roche, Germany). Total VEGFR2 and VEGFR2 phosphorylation was determined by western blotting using 55B11 and 19A10 antibodies (Cell Signaling, Danvers, MA), respectively, at a 1:1000 dilution followed by goat anti-rabbit HorseRadish Peroxidase (HRP) conjugated secondary antibody at 1:20000 dilution (sc-2301, Santa Cruz). The SuperSignal West Femto chemiluminescence (ECL) detection system (Thermo Fisher Scientific, Rockford, IL) was used for detection of immunoreactivity on X-ray films (HyBlot CL; Denville Scientific, Inc. Metuchen, NJ). Experiments were performed in triplicate and results reported as the mean ± 1 standard deviation.

For determination of *in situ* potency, a VEGFR-2 cellular phosphorylation sandwich Enzyme-Linked ImmunoSorbent Assay (ELISA) was utilized (ProQinase, Germany). Primary Human Umbilical Vein Endothelial Cells (HUVECs) were plated in Endothelial Cell Growth Medium (ECGM) supplemented with 10% FBS (PromoCell, Germany), serum starved for 16 hours, incubated with varying concentration of C-furSema for 90 minutes, and then activated with VEGF-A at 100ng/ml for 3 minutes. The level of VEGFR2 phosphorylation was determined via sandwich ELISA using a VEGFR-2 capture antibody and anti-phosphotyrosine detection antibody (PromoCell, Germany). Raw data were converted into percent phosphorylation relative to high and low controls. Cells treated with VEGF-A alone were defined as high control (100%), and those treated with 1 μM sunitinib, a well characterized VEGFR-2 kinase inhibitor with an IC_{50}=10nM, were defined as low control (0%). Inhibition curves were fit using a standard four-parameter sigmoidal curve to yield the $IC_{50.}$ Experiments were performed in duplicate and results reported as the mean ± 1 standard deviation.

Protein expression and purification

Proteins were expressed and purified using established protocols [20]. Briefly, Nrp1-b1b2 (residue 274 to 586) was expressed in *E. coli* and purified using nickel affinity chromatography (IMAC) followed by heparin affinity chromatography. Alkaline Phosphatase (AP) fused VEGF-A was produced from Chinese Hamster Ovary (CHO) cells.

In vitro inhibition assays

Plate-based inhibition assays were performed as previously reported [20]. Briefly, 410 μM *para*-nitrophenol phosphate (p-NPP) hydrolyzed/min/μL of AP-VEGF-A was combined with Sema3F-derived peptides in binding buffer (20 mM Tris, pH 7.5/50 mM NaCl), incubated with Nrp1 affinity plates for 1 hour at 25°C, washed three times with PBS-T (0.01M Phosphate buffered saline, 0.1% Tween 20, pH 7.4), incubated with PBS-T for 5 minutes, aspirated, and developed by addition of 100μL of 1X alkaline phosphatase pNPP substrate [31] followed by quenching with 100μL of 0.5N NaOH. AP activity was quantitatively measured at 405nm using a SpectraMax M5 instrument (Molecular Devices, Sunnyvale, CA). Binding curves were fit using a standard four-parameter sigmoidal curve to yield the IC_{50}. Inhibitory potency is expressed per-subunit for peptides to allow direct

NIH-PA Author Manuscript

NIH-PA Author Manuscript

NIH-PA Author Manuscript

comparison between dimeric and monomeric peptides. Experiments were performed in triplicate and results reported as the mean ± 1 standard deviation. An unpaired t-test was used to compare IC_{50} values.

Circular Dichroism (CD)

C-furSema and C-furSema^{Mon} were dissolved in 0.01M sodium phosphate 50mM NaCl, pH=6.5 at a concentration of 0.5mg/ml. CD spectra were measured using a J-810 spectrapolarimeter (Jasco, Easton, MD) with a 1 mm path length quartz cuvette. All measurements were performed at 25°C and three scans averaged for each spectrum. A blank spectrum was collected in the same manner and used for background subtraction. The fraction of secondary structure was determined by K2D3 using the wavelength range from 200nm to 240nm [32].

Results

C-furSema is a potent inhibitor in situ

To determine the potency of C-furSema function in cellular context, we examined its ability to inhibit VEGF-A mediated activation of VEGFR-2. Nrp1 and VEGFR-2 were stably expressed in PAE cells [30], and the ability of C-furSema to inhibit VEGF-A dependent phosphorylation of VEGFR-2 Y1175 was assessed. C-furSema markedly inhibited VEGF-A dependent VEGFR-2 activation (Figure 1B). To confirm this finding in a distinct cell type, and determine the potency and extent of this inhibition in primary endothelial cells, we measured the dose-dependent inhibitory effect of C-furSema on the activation of VEGFR-2 in HUVEC cells using a quantitative sandwich ELISA. Strikingly, C-furSema showed potent inhibition of VEGFR-2 activation with an IC_{50}=34 ± 15 nM (Figure 1C), consistent with its potency *in vitro* [20], and more than two orders of magnitude greater than short peptide inhibitors of Nrp1 [27, 28, 33, 34]. Additionally, complete inhibition of VEGFR-2 activation was observed in HUVEC cells, in contrast to other Nrp inhibitors that are able to only partially inhibit VEGFR-2 activation even at maximal dose [28]. Thus, C-furSema is a potent inhibitor of Nrp1-dependent activation of endothelial cells *in situ*.

Mechanism of C-furSema potency

C-furSema, which corresponds to the full C-terminal basic domain of Sema3F, is larger and more complex than peptide and peptido-mimetic inhibitors that have been developed to target Nrp1. Given the dimeric nature of C-furSema, due to its conserved inter-molecular disulfide bond, we predicted that the potency of C-furSema might be attributable to avidity effects arising from dual engagement of Nrp1. Indeed, previous studies have demonstrated that oligomeric peptide inhibitors of Nrp have enhanced potency [28].

To test this, we produced a monomeric form of C-furSema by mutating the single conserved cysteine residue responsible for dimerization to serine (C-furSema^{Mon}). The ability of C-furSema and C-furSema^{Mon} to competitively block VEGF-A binding to Nrp1 was compared (Figure 2). A significant decrease in potency was observed for the monomer (black line, IC_{50} = 1.3 ± 0.7 μM) compared to the dimer (grey line, IC_{50} = 24 ± 1 nM). While these data indicate a direct correlation of oligomerization and potency, it is notable that the monomeric species of C-furSema is still an order of magnitude more potent than previously published inhibitors [27, 28, 33, 34], suggesting that additional mechanisms may contribute to C-furSema potency.

A C-terminal arginine has been shown to be critical for Nrp ligand binding [19]. In the Sema3 family, furin processing liberates a C-terminal arginine and is required for Nrp binding [20, 26]. In Nrp1 ligands, residues near the C-terminal arginine have been shown to

NIH-PA Author Manuscript

NIH-PA Author Manuscript

NIH-PA Author Manuscript

contribute to potency and selectivity [22, 35]. Thus, we hypothesized that residues directly upstream of the C-terminus might be responsible for enhanced potency.

To test the role of the C-terminal residues, we performed alanine scanning mutagenesis of the seven C-terminal residues of C-furSema (Figure 3A & B). As expected, mutation of the C-terminal arginine of C-furSema to alanine, R779A, dramatically decreased its inhibition potency by greater than two orders-of-magnitude (IC_{50} = 4.5 ± 0.2 μM). Surprisingly, no other mutation decreased C-furSema potency. In fact, the R778A was slightly more potent, consistent with a recent report of a role for the C-1 position in tuning potency [35]. These data confirm the importance of a C-terminal arginine in Sema3 binding to Nrp1, but indicate that the residues directly upstream minimally contribute to potent competitive binding to Nrp1. Therefore, the enhanced potency of C-furSema relative to other peptide inhibitors cannot be explained by additional interactions within the region directly proximal to the C-terminal arginine.

Contribution of the N-terminal helical region

In addition to the C-terminus, the N-terminal sequence of C-furSema is conserved across species. Furthermore, secondary structure predictions indicate α-helical propensity for the eleven amino acids centered around the cysteine (Figure 4A). Notably, this is the only predicted structured region in the otherwise extended C-terminal basic domain of Sema3. Based on this, we hypothesized that the N-terminus may be involved in binding to Nrp1. To test this, we produced a protein with half of the predicted helix deleted but which retained the conserved cysteine residue necessary and sufficient for dimerization (ΔN-C-furSema). Based on a simple avidity model, ΔN-C-furSema should have unaltered inhibitory potency. Strikingly, ΔN-C-furSema was approximately five-fold less potent than C-furSema (IC_{50} = 111 ± 21 nM and 25 ± 3 nM, respectively) (Figure 4B). These data suggest that the N-terminal region of C-furSema, centered around the conserved cysteine, contributes to potent competitive inhibition of VEGF-A binding to Nrp1. However, this could be due to either direct binding of the N-terminal region to Nrp1 or indirect effects of orienting the two C-terminal arginines for optimal Nrp binding.

The conserved cysteine of C-furSema is required both for oligomerization and potent competitive Nrp1 binding. Interestingly, the cysteine is centered within the predicted N-terminal helix. This led us to examine the possibility of an additional role for the intermolecular disulfide in maintaining the structure of the N-terminal region. Thus, we compared the secondary structure of C-furSema and C-furSema^{Mon} using CD. The overall spectra are consistent with the predicted secondary structure of C-furSema, overall coil with a smaller helical component. The difference spectrum clearly shows a loss of helical character in C-furSema^{Mon} (Figure 4C). Fitting the individual spectra reveals an approximately 30% loss in helicity in C-furSema^{Mon}, with 16% overall helical composition for C-furSema compared to 11% for C-furSema^{Mon}. These data indicate that the conserved cysteine that forms the key intermolecular disulfide in Sema3F is not only important for determining the oligomeric state of C-furSema but also in stabilizing the N-terminal helical region of C-furSema required for potent engagement of Nrp1.

We interpret these data to indicate that the disulfide stabilized N-terminal helix directly contributes to Nrp1 binding. However, it remains possible that this region indirectly affects potency by imposing conformational constraints that orient the C-furSema dimer. To distinguish between these possibilities, we designed a heterodimer composed of one subunit of C-furSema and one subunit containing only the thirteen N-terminal helical residues (C-furSema^{Het}) (Figure 5A). This construct contains the full N-terminal helix but only a single C-terminal arginine. This unique disulfide linked heterodimer was produced and purified to >95% purity (Figure 5B). Strikingly, C-furSema^{Het} was as potent as C-furSema at inhibiting

NIH-PA Author Manuscript

NIH-PA Author Manuscript

NIH-PA Author Manuscript

VEGF-A-dependent activation of endothelial cells (Figure 5C) and VEGF-A binding to Nrp1 (Figure 5D, IC_{50} = 35 ± 3 nM and 24 ± 1 nM, respectively). This is in stark contrast to C-furSema^{Mon}, with an IC_{50} = 1.3 ± 0.7 μM (Figure 5D). These data emphasize the importance of the N-terminal helical region and demonstrate that C-furSema potency is determined by a hetero-bivalent mechanism combining a C-terminal arginine and structured N-terminal helical region.

Insights into distinctly furin processed forms of Sema3A

This raises the question of whether the distance between C-terminal arginine and helical region is a critical factor in determining Sema3 engagement of Nrp1. There are between one and three furin cleavage sites in the C-terminal basic domain of different Sema3 family members, which produce natural variants with different spacing between C-terminal arginine and the dimeric helical region. While Sema3F possesses one furin consensus site, Sema3A possesses three. These three sites in Sema3A are known to be processed and important for function [26] (Figure 6). To define the role of the multiple furin processing sites in Sema3A, we measured the inhibitory potency of the three processed variants of Sema3A. The furin processed forms similar to C-furSema, Sema3A.2 and Sema3A.3, are similar in potency (Figure 6B, IC_{50} = 45 ± 12 nM and 27 ± 5 nM, respectively). Intriguingly, the shortest form, Sema3A.1 shows significantly reduced potency (IC_{50} = 1.1 ± 0.3 μM). This form has the same amino acid sequence in both helical and C-terminal motifs, differing only in the spacing of these motifs. These data suggest that furin site selection may represent a natural mechanism to produce Sema3A proteins with differing Nrp binding motif spacing, providing a unique mechanism for fine-tuning Sema3A/Nrp1 binding.

Discussion

Together, these data demonstrate that Sema3 family members engage Nrp1 utilizing two distinct regions in their C-terminal domain, a C-terminal arginine and upstream helical region. This engagement results in potent competitive binding to Nrp1 that antagonizes VEGF binding and cellular activation. Importantly, the decreased potency observed between dimeric and monomeric forms of C-furSema is primarily due not to the presence of two C-terminal arginine motifs, but instead the presence of the stable helical motif, as demonstrated by the potency of C-furSema^{Het}. These data indicate that the potent competitive binding of C-furSema to Nrp1 is determined by a unique hetero-bivalent mechanism requiring only one C-terminal arginine and the novel upstream helical region.

Previously, it has been shown that the exon seven encoded residues of VEGF-A engage the L1 loop of the Nrp1 b1 domain, enhancing binding and controlling Nrp1 receptor selectivity [22]. In contrast, the L1 loop of Nrp1/2 does not play a role in selective Sema3 binding [36]. Our current data demonstrate that Sema3s utilize its upstream helical motif to enable potent hetero-bivalent engagement of Nrp. The physical location of the Sema3 helical binding site on Nrp1 is an important future direction for both mechanistic insights into Sema3 function and inhibitor design. It is notable that Sema3A.1 possesses only four residues between the N-terminal helical region and the C-terminal arginine and has significantly reduced potency, indicating a minimal length is required to tether these two physically distinct sites. Thus, VEGF and Sema3 utilize both common and unique mechanisms to engage Nrp1.

Since Nrp has critical roles in pathological angiogenesis and aberrant axon guidance, significant effort has been devoted to producing Nrp inhibitors. Peptide and small molecule inhibitors have been produced against the C-terminal arginine binding pocket, but generally possess modest (μM) potency [28, 33, 34, 37]. We demonstrate that by coupling inhibitor oligomerization with covalent tethering of the helical and C-terminal arginine binding motif,

NIH-PA Author Manuscript

NIH-PA Author Manuscript

NIH-PA Author Manuscript

a two order-of-magnitude gain in inhibitory potency can be achieved. The identification of two distinct Nrp1 binding sites that, when tethered together, produce a potent inhibitor presents exciting possibilities for fragment-based design strategies combining existing inhibitors of the C-terminal arginine binding pocket with novel helical motif binding site inhibitors.

The physiological role of furin processing in the regulation of Sema3 signaling, as opposed to inhibition of VEGF binding, remains to be determined. While inhibition only requires avid binding to a single Nrp receptor, Sema3 signaling minimally requires engagement of two receptor molecules and assembly of the signaling complex. Our data indicate that, at a minimum, furin processing is required to activate Sema3 for Nrp b1-domain binding by liberation of a C-terminal arginine. Importantly, C-furSema^{Het} maintains potent engagement of Nrp, suggesting that furin processing of a single subunit of the Sema3 dimer may be sufficient for potent activation. Alternatively, furin processing may effect Sema3 engagement of the Nrp b1 domain quantitatively such that the different forms have progressively increasing signal potency from unprocessed to singly processed to dual processed.

Sema3 engagement of Nrp is more complex than VEGF in that two distinct domains are required. Both Sema3 C-terminal domain binding to the Nrp b1 domain and Sema3 Sema domain binding to the Nrp a1 domain are important for Sema3 signaling [38, 39]. Recent structural work has provided significant insight into the contribution of the Nrp a1 domain in Sema3 binding [40] and assembly of the active Sema3/Plexin/Nrp complex [41]. The specific contribution of a1 and b1 domains in terms of binding potency, specificity, and coupling between the two interacting domains is an active area of research [6].

The ability of Sema3 to engage the Nrp b1-domain has clear implications for Sema3 signaling in the nervous system but also in the cardiovascular systems. For example Sema3A, which is critical for nervous system development [42], has been shown to inhibit VEGF-dependent angiogenesis, yet acts as a vascular permeability factor [12]. Inhibition of VEGF is consistent with our data demonstrating direct competition for Nrp binding. However, induction of vascular permeability by Sema3 was found to be due to specific Nrp-dependent signaling rather than competitive binding. It is possible that these two functions of Sema3 in the cardiovascular systems are differentially regulated by furin processing. Indeed, furin processing of Sema3 family members may have significant physiological implications for regulated function in both nervous and cardiovascular systems [1].

Our data demonstrate that the furin cleavage sites in the C-terminal domain of Sema3A are non-equivalent in terms of receptor binding. Thus, C-terminal furin processing functions not only as a binary activation mechanism but can produce activated species with differing physical properties. Recent data indicate that this may have profound physiological implications. Mutations of two different residues in the Sema3A.1 furin site, R730Q and R733H, have recently been shown to cause Kallmann's syndrome, a serious genetic disease resulting from aberrant Sema3A dependent axon guidance [43]. Thus, differential furin processing of the C-terminal domain of Sema3 can have profound functional and physiological effects in human disease. Combined with these mechanistic insights, discovery of these disease associated mutations underline the importance of future studies of the regulation and function of differential furin processing of Sema3 in regulating Nrp engagement in both neuronal and cardiovascular signaling.

Acknowledgments

This study was supported by NIH grants R01GM094155 (C.W.V.K.), T32HL072743 (M. W. P.), P20GM103486 (Core support) and the Kentucky Lung Cancer Research Program.

NIH-PA Author Manuscript

NIH-PA Author Manuscript

NIH-PA Author Manuscript

We thank Drs Matthew Gentry and David Rodgers, and David Meekins for helpful discussions.

Abbreviations

AP	alkaline phosphatase
HUVEC	human umbilical vein endothelial cells
PAE	porcine aortic endothelial
Nrp1	Neuropilin-1
Sema3A-3G	Semaphorin 3A-3G
C-furSema	furin-processed C-terminal domain of Sema3F
VEGF-A	vascular endothelial growth factor-A
VEGFR-2	vascular endothelial growth factor receptor 2
PBS	phosphate buffered saline
FBS	fetal bovine serum
EBM-2	endothelial cell basal growth medium-2
HRP	horseradish peroxidase
ECL	enhanced chemiluminescence
ELISA	enzyme-linked immunosorbent assay
ECGM	endothelial cell growth medium
IMAC	nickel affinity chromatography
CHO	Chinese hamster ovary
pNPP	*para*-nitrophenol phosphate
HPLC	high-performance liquid chromatography
CD	circular dichroism

References

1. Parker MW, Guo HF, Li X, Linkugel AD, Vander Kooi CW. Function of members of the neuropilin family as essential pleiotropic cell surface receptors. Biochemistry. 2012; 51:9437–9446. [PubMed: 23116416]
2. Geretti E, Shimizu A, Klagsbrun M. Neuropilin structure governs VEGF and semaphorin binding and regulates angiogenesis. Angiogenesis. 2008; 11:31–39. [PubMed: 18283547]
3. Pellet-Many C, Frankel P, Jia H, Zachary I. Neuropilins: structure, function and role in disease. Biochem J. 2008; 411:211–226. [PubMed: 18363553]
4. de Wit J, Verhaagen J. Role of semaphorins in the adult nervous system. Progress in neurobiology. 2003; 71:249–267. [PubMed: 14687984]
5. Gu C, Giraudo E. The role of semaphorins and their receptors in vascular development and cancer. Exp Cell Res. 2013; 319:1306–1316. [PubMed: 23422037]
6. Hota PK, Buck M. Plexin structures are coming: opportunities for multilevel investigations of semaphorin guidance receptors, their cell signaling mechanisms, and functions. Cell Mol Life Sci. 2012; 69:3765–3805. [PubMed: 22744749]
7. Futamura M, Kamino H, Miyamoto Y, Kitamura N, Nakamura Y, Ohnishi S, Masuda Y, Arakawa H. Possible role of semaphorin 3F, a candidate tumor suppressor gene at 3p21.3, in p53-regulated tumor angiogenesis suppression. Cancer Res. 2007; 67:1451–1460. [PubMed: 17308083]

NIH-PA Author Manuscript NIH-PA Author Manuscript NIH-PA Author Manuscript

8. Gaur P, Bielenberg DR, Samuel S, Bose D, Zhou Y, Gray MJ, Dallas NA, Fan F, Xia L, Lu J, Ellis LM. Role of class 3 semaphorins and their receptors in tumor growth and angiogenesis. Clin Cancer Res. 2009; 15:6763–6770. [PubMed: 19887479]
9. Joyal JS, Sitaras N, Binet F, Rivera JC, Stahl A, Zaniolo K, Shao Z, Polosa A, Zhu T, Hamel D, Djavari M, Kunik D, Honore JC, Picard E, Zabeida A, Varma DR, Hickson G, Mancini J, Klagsbrun M, Costantino S, Beausejour C, Lachapelle P, Smith LE, Chemtob S, Sapieha P. Ischemic neurons prevent vascular regeneration of neural tissue by secreting semaphorin 3A. Blood. 2011; 117:6024–6035. [PubMed: 21355092]
10. Buehler A, Sitaras N, Favret S, Bucher F, Berger S, Pielen A, Joyal JS, Juan AM, Martin G, Schlunck G, Agostini HT, Klagsbrun M, Smith LE, Sapieha P, Stahl A. Semaphorin 3F forms an anti-angiogenic barrier in outer retina. FEBS letters. 2013; 587:1650–1655. [PubMed: 23603393]
11. Fukushima Y, Okada M, Kataoka H, Hirashima M, Yoshida Y, Mann F, Gomi F, Nishida K, Nishikawa S, Uemura A. Sema3E-PlexinD1 signaling selectively suppresses disoriented angiogenesis in ischemic retinopathy in mice. The Journal of clinical investigation. 2011; 121:1974–1985. [PubMed: 21505259]
12. Acevedo LM, Barillas S, Weis SM, Gothert JR, Cheresh DA. Semaphorin 3A suppresses VEGF-mediated angiogenesis yet acts as a vascular permeability factor. Blood. 2008; 111:2674–2680. [PubMed: 18180379]
13. Sekido Y, Bader S, Latif F, Chen JY, Duh FM, Wei MH, Albanesi JP, Lee CC, Lerman MI, Minna JD. Human semaphorins A(V) and IV reside in the 3p21.3 small cell lung cancer deletion region and demonstrate distinct expression patterns. Proc Natl Acad Sci U S A. 1996; 93:4120–4125. [PubMed: 8633026]
14. Capparuccia L, Tamagnone L. Semaphorin signaling in cancer cells and in cells of the tumor microenvironment--two sides of a coin. J Cell Sci. 2009; 122:1723–1736. [PubMed: 19461072]
15. Potiron VA, Roche J, Drabkin HA. Semaphorins and their receptors in lung cancer. Cancer Lett. 2009; 273:1–14. [PubMed: 18625544]
16. Bielenberg DR, Hida Y, Shimizu A, Kaipainen A, Kreuter M, Kim CC, Klagsbrun M. Semaphorin 3F, a chemorepulsant for endothelial cells, induces a poorly vascularized, encapsulated, nonmetastatic tumor phenotype. The Journal of clinical investigation. 2004; 114:1260–1271. [PubMed: 15520858]
17. Kessler O, Shraga-Heled N, Lange T, Gutmann-Raviv N, Sabo E, Baruch L, Machluf M, Neufeld G. Semaphorin-3F is an inhibitor of tumor angiogenesis. Cancer Res. 2004; 64:1008–1015. [PubMed: 14871832]
18. Castro-Rivera E, Ran S, Thorpe P, Minna JD. Semaphorin 3B (SEMA3B) induces apoptosis in lung and breast cancer, whereas VEGF165 antagonizes this effect. Proc Natl Acad Sci U S A. 2004; 101:11432–11437. [PubMed: 15273288]
19. Vander Kooi CW, Jusino MA, Perman B, Neau DB, Bellamy HD, Leahy DJ. Structural basis for ligand and heparin binding to neuropilin B domains. Proc Natl Acad Sci U S A. 2007; 104:6152–6157. [PubMed: 17405859]
20. Parker MW, Hellman LM, Xu P, Fried MG, Vander Kooi CW. Furin processing of semaphorin 3F determines its anti-angiogenic activity by regulating direct binding and competition for neuropilin. Biochemistry. 2010; 49:4068–4075. [PubMed: 20387901]
21. Delcombel R, Janssen L, Vassy R, Gammons M, Haddad O, Richard B, Letourneur D, Bates D, Hendricks C, Waltenberger J, Starzec A, Sounni NE, Noel A, Deroanne C, Lambert C, Colige A. New prospects in the roles of the C-terminal domains of VEGF-A and their cooperation for ligand binding, cellular signaling and vessels formation. Angiogenesis. 2013; 16:353–371. [PubMed: 23254820]
22. Parker MW, Xu P, Li X, Vander Kooi CW. Structural basis for the selective vascular endothelial growth factor-A (VEGF-A) binding to neuropilin-1. J Biol Chem. 2012
23. Varshavsky A, Kessler O, Abramovitch S, Kigel B, Zaffryar S, Akiri G, Neufeld G. Semaphorin-3B is an angiogenesis inhibitor that is inactivated by furin-like pro-protein convertases. Cancer Res. 2008; 68:6922–6931. [PubMed: 18757406]

NIH-PA Author Manuscript NIH-PA Author Manuscript NIH-PA Author Manuscript

24. Casazza A, Kigel B, Maione F, Capparuccia L, Kessler O, Giraudo E, Mazzone M, Neufeld G, Tamagnone L. Tumour growth inhibition and anti-metastatic activity of a mutated furin-resistant Semaphorin 3E isoform. EMBO molecular medicine. 2012; 4:234–250. [PubMed: 22247010]
25. Christensen C, Ambartsumian N, Gilestro G, Thomsen B, Comoglio P, Tamagnone L, Guldberg P, Lukanidin E. Proteolytic processing converts the repelling signal Sema3E into an inducer of invasive growth and lung metastasis. Cancer Res. 2005; 65:6167–6177. [PubMed: 16024618]
26. Adams RH, Lohrum M, Klostermann A, Betz H, Puschel AW. The chemorepulsive activity of secreted semaphorins is regulated by furin-dependent proteolytic processing. EMBO J. 1997; 16:6077–6086. [PubMed: 9321387]
27. Starzec A, Vassy R, Martin A, Lecouvey M, Di Benedetto M, Crepin M, Perret GY. Antiangiogenic and antitumor activities of peptide inhibiting the vascular endothelial growth factor binding to neuropilin-1. Life Sci. 2006; 79:2370–2381. [PubMed: 16959272]
28. von Wronski MA, Raju N, Pillai R, Bogdan NJ, Marinelli ER, Nanjappan P, Ramalingam K, Arunachalam T, Eaton S, Linder KE, Yan F, Pochon S, Tweedle MF, Nunn AD. Tuftsin binds neuropilin-1 through a sequence similar to that encoded by exon 8 of vascular endothelial growth factor. J Biol Chem. 2006; 281:5702–5710. [PubMed: 16371354]
29. Teesalu T, Sugahara KN, Kotamraju VR, Ruoslahti E. C-end rule peptides mediate neuropilin-1-dependent cell, vascular, and tissue penetration. Proc Natl Acad Sci U S A. 2009; 106:16157–16162. [PubMed: 19805273]
30. Becker PM, Waltenberger J, Yachechko R, Mirzapoiazova T, Sham JS, Lee CG, Elias JA, Verin AD. Neuropilin-1 regulates vascular endothelial growth factor-mediated endothelial permeability. Circ Res. 2005; 96:1257–1265. [PubMed: 15920019]
31. Jardin BA, Zhao Y, Selvaraj M, Montes J, Tran R, Prakash S, Elias CB. Expression of SEAP (secreted alkaline phosphatase) by baculovirus mediated transduction of HEK 293 cells in a hollow fiber bioreactor system. Journal of biotechnology. 2008; 135:272–280. [PubMed: 18499293]
32. Louis-Jeune C, Andrade-Navarro MA, Perez-Iratxeta C. Prediction of protein secondary structure from circular dichroism using theoretically derived spectra. Proteins: Structure, Function, and Bioinformatics. 2012; 80:374–381.
33. Jarvis A, Allerston CK, Jia H, Herzog B, Garza-Garcia A, Winfield N, Ellard K, Aqil R, Lynch R, Chapman C, Hartzoulakis B, Nally J, Stewart M, Cheng L, Menon M, Tickner M, Djordjevic S, Driscoll PC, Zachary I, Selwood DL. Small molecule inhibitors of the neuropilin-1 vascular endothelial growth factor A (VEGF-A) interaction. J Med Chem. 2010; 53:2215–2226. [PubMed: 20151671]
34. Jia H, Bagherzadeh A, Hartzoulakis B, Jarvis A, Lohr M, Shaikh S, Aqil R, Cheng L, Tickner M, Esposito D, Harris R, Driscoll PC, Selwood DL, Zachary IC. Characterization of a bicyclic peptide neuropilin-1 (NP-1) antagonist (EG3287) reveals importance of vascular endothelial growth factor exon 8 for NP-1 binding and role of NP-1 in KDR signaling. J Biol Chem. 2006; 281:13493–13502. [PubMed: 16513643]
35. Parker MW, Linkugel AD, Vander Kooi CW. Effect of C-terminal Sequence on Competitive Semaphorin Binding to Neuropilin-1. J Mol Biol. 2013
36. Parker MW, Xu P, Guo HF, Vander Kooi CW. Mechanism of selective VEGF-A binding by neuropilin-1 reveals a basis for specific ligand inhibition. PLoS One. 2012; 7:e49177. [PubMed: 23145112]
37. Binetruy-Tournaire R, Demangel C, Malavaud B, Vassy R, Rouyre S, Kraemer M, Plouet J, Derbin C, Perret G, Mazie JC. Identification of a peptide blocking vascular endothelial growth factor (VEGF)-mediated angiogenesis. EMBO J. 2000; 19:1525–1533. [PubMed: 10747021]
38. Gu C, Limberg BJ, Whitaker GB, Perman B, Leahy DJ, Rosenbaum JS, Ginty DD, Kolodkin AL. Characterization of neuropilin-1 structural features that confer binding to semaphorin 3A and vascular endothelial growth factor 165. J Biol Chem. 2002; 277:18069–18076. [PubMed: 11886873]
39. Koppel AM, Feiner L, Kobayashi H, Raper JA. A 70 amino acid region within the semaphorin domain activates specific cellular response of semaphorin family members. Neuron. 1997; 19:531–537. [PubMed: 9331346]

NIH-PA Author Manuscript

NIH-PA Author Manuscript

NIH-PA Author Manuscript

40. Appleton BA, Wu P, Maloney J, Yin J, Liang WC, Stawicki S, Mortara K, Bowman KK, Elliott JM, Desmarais W, Bazan JF, Bagri A, Tessier-Lavigne M, Koch AW, Wu Y, Watts RJ, Wiesmann C. Structural studies of neuropilin/antibody complexes provide insights into semaphorin and VEGF binding. EMBO J. 2007; 26:4902–4912. [PubMed: 17989695]

41. Janssen BJ, Malinauskas T, Weir GA, Cader MZ, Siebold C, Jones EY. Neuropilins lock secreted semaphorins onto plexins in a ternary signaling complex. Nat Struct Mol Biol. 2012; 19:1293–1299. [PubMed: 23104057]

42. Pasterkamp RJ. Getting neural circuits into shape with semaphorins. Nature reviews Neuroscience. 2012; 13:605–618.

43. Hanchate NK, Giacobini P, Lhuillier P, Parkash J, Espy C, Fouveaut C, Leroy C, Baron S, Campagne C, Vanacker C, Collier F, Cruaud C, Meyer V, Garcia-Pinero A, Dewailly D, Cortet-Rudelli C, Gersak K, Metz C, Chabrier G, Pugeat M, Young J, Hardelin JP, Prevot V, Dode C. SEMA3A, a gene involved in axonal pathfinding, is mutated in patients with Kallmann syndrome. PLoS genetics. 2012; 8:e1002896. [PubMed: 22927827]

NIH-PA Author Manuscript

NIH-PA Author Manuscript

NIH-PA Author Manuscript

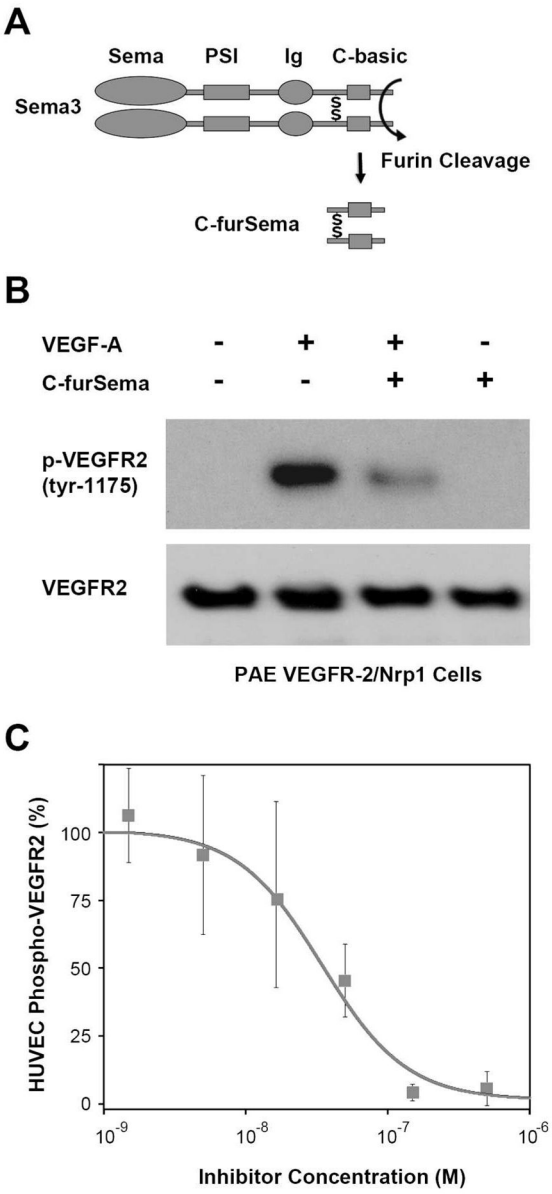

Figure 1.

C-furSema potently inhibits VEGF-A mediated VEGFR2 activation *in situ*. A) A schematic representation of Sema3 highlighting the furin-processed C-terminal domain (C-furSema). B) Activation of PAE cells stably overexpressing Nrp1 and VEGFR2 by VEGF-A is inhibited by C-furSema as demonstrated by a decrease in VEGFR-2 Tyr-1175 auto-phosphorylation. C) C-furSema is a potent dose-dependent inhibitor of VEGF-A mediated HUVEC activation as demonstrated by sandwich ELISA (IC_{50} = 34 ± 15 nM). Phospho-VEGFR-2 levels were normalized to VEGF-A alone and 1 μM sunitinib.

NIH-PA Author Manuscript

NIH-PA Author Manuscript

NIH-PA Author Manuscript

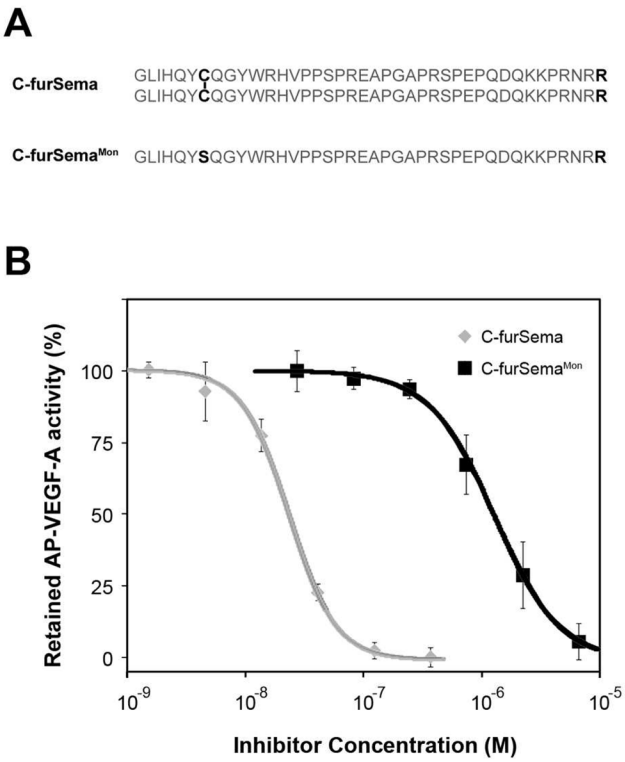

Figure 2.

Effect of the intermolecular disulfide on C-furSema potency. A) Comparison of dimeric C-furSema and C-furSema^{Mon} B) reveals a critical role for the conserved inter-molecular disulfide C-furSema (grey line, IC_{50} = 24 ± 1 nM) and C-furSema^{Mon} (black line, IC_{50} = 1.3 ± 0.7 μM) in inhibiting VEGF-A binding to Nrp1.

NIH-PA Author Manuscript

NIH-PA Author Manuscript

NIH-PA Author Manuscript

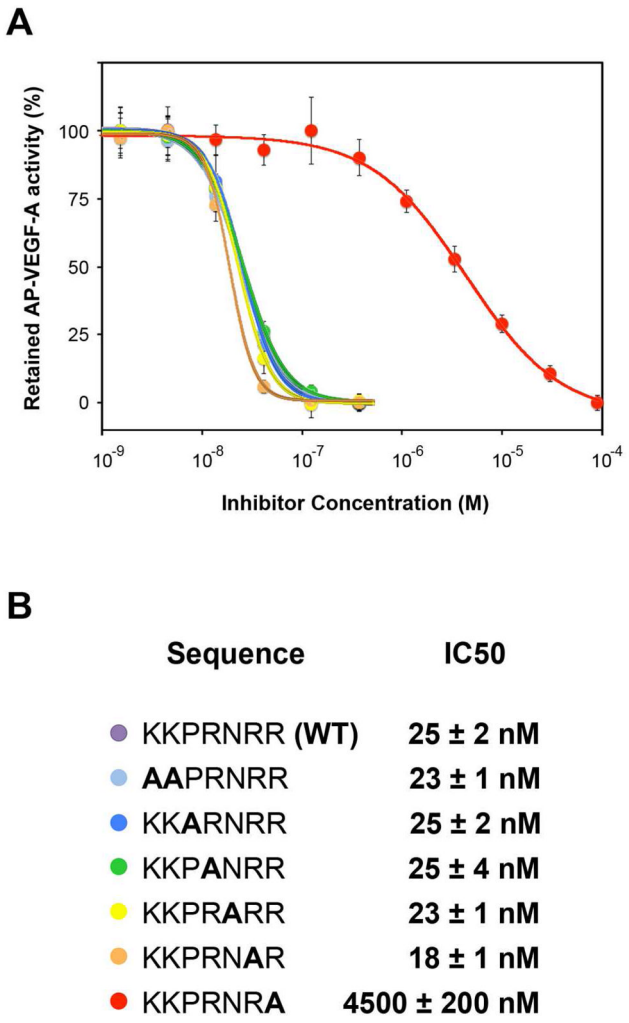

Figure 3.

C-furSema C-terminal arginine contributes to high affinity binding to Nrp. A) An alanine scan of the C-terminus of C-furSema was performed. The ability of C-furSema and mutants to inhibit AP-VEGF-A binding to Nrp1 was determined. B) Inhibition curves were utilized to determine peptide potency (IC_{50}), with a significant decrease only observed with the C-terminal arginine mutant.

NIH-PA Author Manuscript

NIH-PA Author Manuscript

NIH-PA Author Manuscript

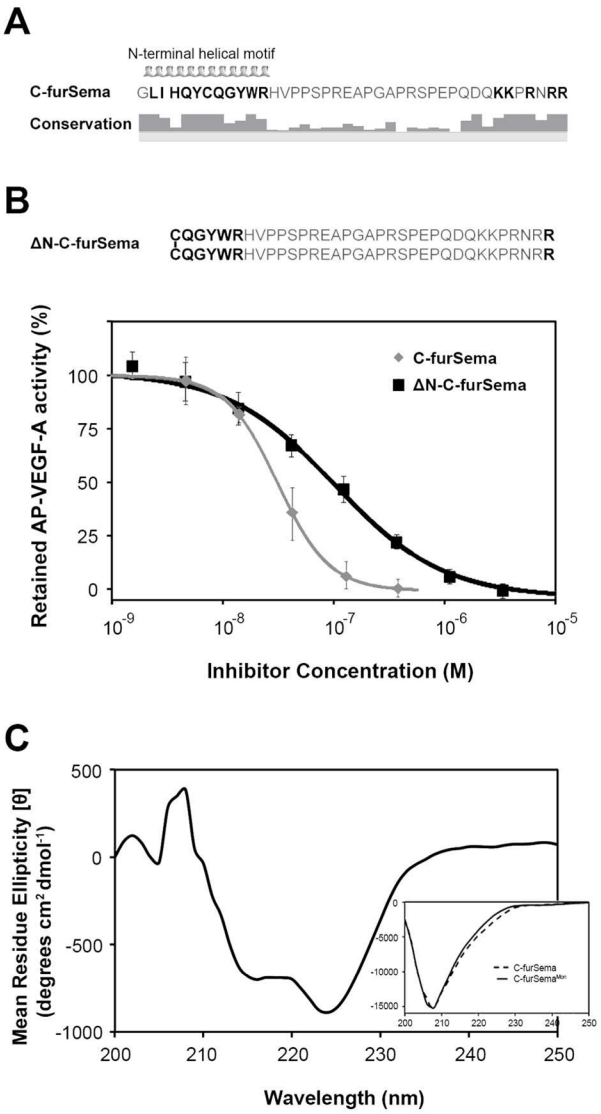

Figure 4.

The N-terminal helical motif is a structured region that contributes to potency. A) Sequence, predicted secondary structure, and conservation of C-furSema (based on an alignment of human, rat, mouse, cow, dog, chicken, and zebrafish orthologs). B) ΔN-C-furSema, a N-terminal helical deletion decreases the potency of C-furSema (IC_{50} = 111 ± 21 nM vs. 25 ± 3 nM, respectively). C) Difference CD spectrum of dimeric versus monomeric C-furSema reveals a characteristic loss in α-helical content. (Inset) CD spectra of dimeric C-furSema (dashed line) and C-furSema3^{Mon} (solid line).

NIH-PA Author Manuscript

NIH-PA Author Manuscript

NIH-PA Author Manuscript

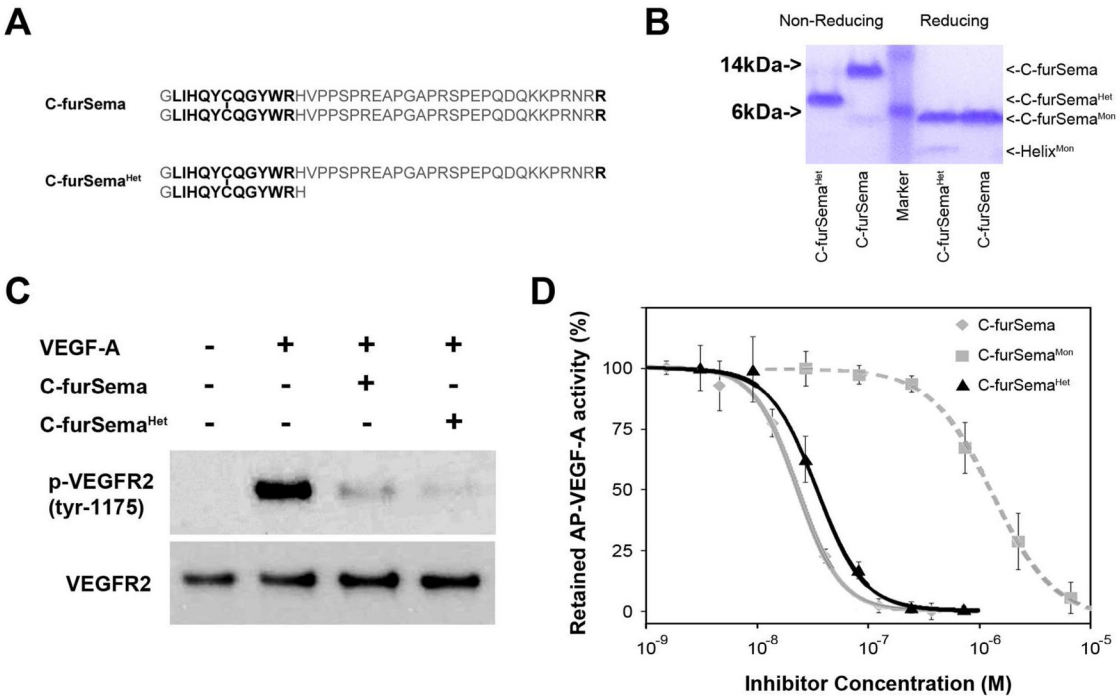

Figure 5.

The helical motif determines potent competitive Nrp1 binding. A) To determine the contribution of N-terminal helical region in mediating Nrp inhibition, C-furSema^{Het} was synthesized. B) Comparison of non-reducing versus reducing SDS-PAGE demonstrates the purity and correct intermolecular disulfide bond formation of C-furSema and C-furSema^{Het}. C) C-furSema and C-furSema^{Het} equivalently inhibit VEGF-A dependent activation of PAE cells and D) have nearly equal potencies, IC_{50} = 24 ± 1 nM vs. IC_{50} = 35 ± 3 nM, respectively.

NIH-PA Author Manuscript

NIH-PA Author Manuscript

NIH-PA Author Manuscript

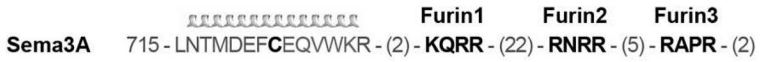

Isoforms	IC_{50}
Sema3A.1	1100 ± 300 nM
Sema3A.2	45 ± 12 nM
Sema3A.3	27 ± 5 nM

Figure 6.

Differential furin processing of Sema3A. Sema3A possesses a disulfide bonded dimeric helical motif followed by three furin consensus (RXXR) sites. These three distinct furin processing sites produce C-terminal domains of significantly different length and potencies.